AGU PUBLICATIONS

JGR

Journal of Geophysical Research: Oceans

RESEARCH ARTICLE

10.1002/2015JC011522

Key Points:
- Local mixing fostered by flow instabilities induces long-term, positive thermohaline trends in the bottom of the southern Adriatic Sea
- Only exceptional production and sinking of large amounts of very dense shelf water can cause drastic bottom water renewal
- The hypothesized saw-tooth modulation of the deep-water thermohaline properties could be observed in similar basins in the world ocean

Supporting Information:
- Supporting Information S1
- Movie S1

Correspondence to:
S. Querin,
squerin@inogs.it

Citation:
Querin, S., M. Bensi, V. Cardin, C. Solidoro, S. Bacer, L. Mariotti, F. Stel, and V. Malačič (2016), Saw-tooth modulation of the deep-water thermohaline properties in the southern Adriatic Sea, *J. Geophys. Res. Oceans*, *121*, doi:10.1002/2015JC011522.

Received 2 DEC 2015
Accepted 31 MAY 2016
Accepted article online 2 JUN 2016

Saw-tooth modulation of the deep-water thermohaline properties in the southern Adriatic Sea

Stefano Querin[1], Manuel Bensi[1], Vanessa Cardin[1], Cosimo Solidoro[1], Sara Bacer[2,3], Laura Mariotti[2], Fulvio Stel[4], and Vlado Malačič[5]

[1]Istituto Nazionale di Oceanografia e di Geofisica Sperimentale, Trieste, Italy, [2]International Centre for Theoretical Physics, Trieste, Italy, [3]Atmospheric Chemistry Department, Max Planck Institute for Chemistry, Mainz, Germany, [4]Agenzia Regionale per la Protezione dell'Ambiente del Friuli-Venezia Giulia - Centro Regionale di Modellistica Ambientale, Udine, Italy, [5]National Institute of Biology - Marine Biology Station, Piran, Slovenia

Abstract In this study, we investigate the dynamics of the bottom layer of the southern Adriatic Sea (eastern Mediterranean basin) by merging experimental measurements and numerical simulations. We hypothesize that the recently observed continuous density decrease over time, which was basically related to a temperature increase, and the following sudden density rise, which was caused by the intrusion of very dense water masses (cold but relatively fresh), constitute one cycle of a general "saw-tooth" pattern: the alternation of long-lasting and almost linear density decreases (mixing phases) and sudden density increases (dense water intrusion phases). The model results, which provide a basin-scale view of the process, corroborate this theory because they satisfactorily reproduced the observed oceanographic features. We describe the almost linear density decrease in terms of local mixing fostered by the advection of flow instabilities that originate from the large-scale quasi-permanent cyclonic circulation. Conversely, diffusive processes play a minor role in determining the bottom layer thermohaline variability. The interpretation of the experimental findings, supported by the numerical simulations, suggests that similar dynamics might be observed in other basins characterized by similar bathymetric and hydrodynamic features.

1. Introduction

The Adriatic Sea, which is a semienclosed marginal sea in the eastern Mediterranean (Figure 1), is one of several dense water formation sites in the world ocean [*Robinson et al.*, 2001]. After its generation and spreading, Adriatic dense water eventually flows through the Strait of Otranto and sinks in the deepest layers of the Ionian Sea [*Hainbucher et al.*, 2006; *Manca et al.*, 2006], maintaining the eastern Mediterranean thermohaline cell.

Adriatic dense water is formed under favorable winter conditions both on the northern shelf [*Malanotte-Rizzoli*, 1991] and in the southern subbasin [*Ovchinnikov et al.*, 1985]. The meteorological (surface wind stress and buoyancy fluxes) and oceanographic (large-scale circulation) conditions of the Adriatic Sea govern the interannual variability of the northern and southern Adriatic dense water properties and their production rates [*Cardin and Gačić*, 2003; *Mantziafou and Lascaratos*, 2008; *Querin et al.*, 2013].

Northern adriatic dense water (NAdDW), once produced on the shelf, flows southeastward as a bottom-arrested density current. The densest part of the NAdDW first fills the central Adriatic Pit and then sinks in the southern Adriatic Sea along the shelf break until it reaches its equilibrium depth (neutral buoyancy). Typically, a newly formed NAdDW vein can sink to the bottom of the southern Adriatic Pit (SAP) 2–4 months after its generation [*Vilibić*, 2003; *Turchetto et al.*, 2007; *Querin et al.*, 2013]; the "new" dense water uplifts the local, "old" and lighter water, ventilating the bottom layer [*Rubino et al.*, 2012].

Adriatic dense water (AdDW) is instead formed through open-ocean convection in the southern Adriatic Sea. This process mixes fresher and colder surface waters with saltier and warmer waters from the Ionian Sea that are located approximately between depths of 200 and 600 m [*Gačić et al.*, 2002; *Mantziafou and Lascaratos*, 2008]. Heat and salt contributions from the Ionian Sea [*Manca et al.*, 2002; *Gačić et al.*, 2010; *Cardin et al.*, 2011] and, to a lesser degree, from the northern Adriatic [*Wang et al.*, 2006; *Oddo and Guarnieri*, 2011; *Rubino et al.*, 2012] influence the stability of the water column. Hence, the interannual variabilities in

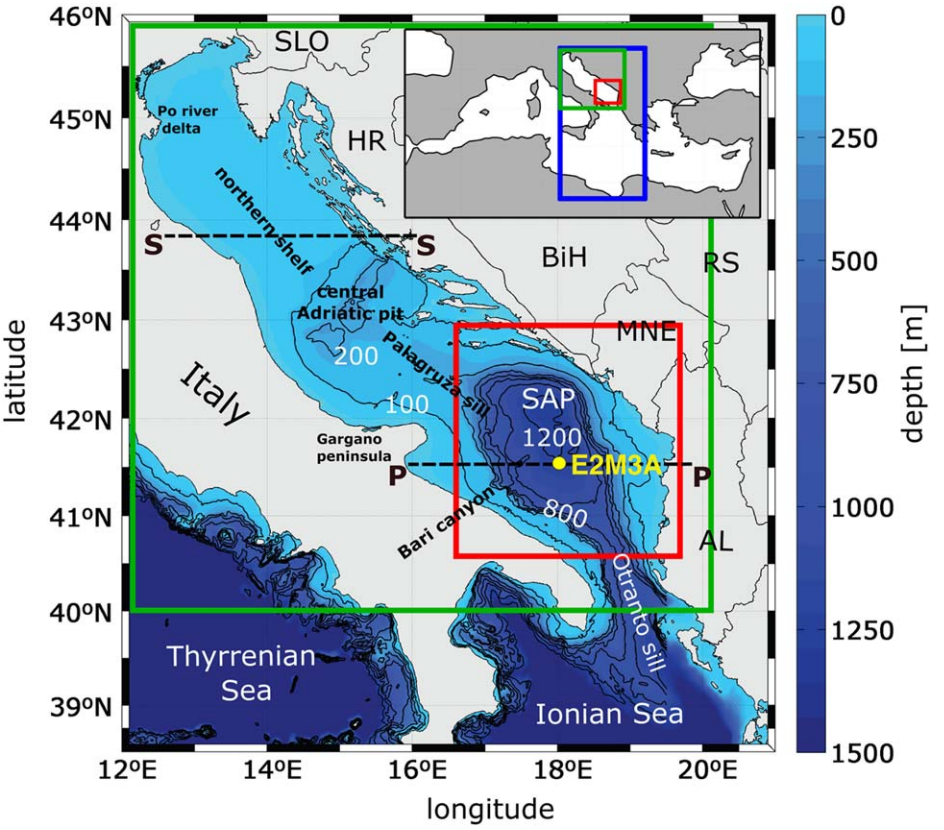

Figure 1. Coastal and bathymetric map of the Adriatic Sea. The yellow symbol marks the position of the E2M3A deep-ocean observatory. The zonal dashed lines S-S and P-P show the vertical transects considered in section 3.2.2 and Figures 4 and 6, respectively. Several morphological features cited in the text are also shown. Insert: map of the Mediterranean Sea. The blue, green, and red boxes indicate the domain of the ADIOS (1/32°), Adriatic Sea (1/32°), and southern Adriatic Sea (1/64°) models, respectively.

the densities, volumes and maximum depths reached by the NAdDW and AdDW in the SAP depend on the variability in the water column thermohaline properties and on the intensity of the winter meteorological forcing over the Adriatic Sea [*Cardin and Gačić*, 2003; *Mantziafou and Lascaratos*, 2008; *Querin et al*., 2013].

Convective mixing in the SAP has rarely involved the deep layer (down to 1000 m depth), and it has never reached the bottom (1250 m) in the last two decades [*Cardin and Gačić*, 2003; *Bensi et al*., 2014]. Moreover, the deepest layer of the SAP (below 1000 m depth) is a restricted area surrounded by two shallower sills, the Palagruža (180 m deep) and the Otranto (800 m deep) sills, on its northern and southern sides, respectively (Figure 1). This geographic confinement creates a natural bathymetric barrier to the horizontal advection of water masses from adjacent subbasins. The layer between 800 and 1000 m is a sort of "buffer layer" that decouples the circulation above 800 m depth from the deepest layer of the SAP, which can be viewed as a "separate" system [*Cardin et al*., 2011]. Because the water entering the southern Adriatic from the Ionian Sea through the Otranto Strait is saltier and warmer (overall lighter) than that in the SAP, the renewal of its bottom layer can be ascribed only to intrusions of very dense water masses formed on the northern Adriatic shelf.

Although rapid renewals of near-bottom layers by dense water intrusions have been studied for decades in several areas of the world ocean (e.g., the polar regions, Atlantic Ocean, and Mediterranean Sea), the slow recovery of the thermohaline properties through mixing and diffusion is less clear and can be ascribed to several processes (e.g., mesoscale and submesoscale turbulence, internal wave breaking, double diffusion, and boundary mixing). A recent modeling study by *Holtermann et al*. [2014] identified and reproduced the main energy sources for deep water boundary mixing in the Baltic Sea (i.e., near-inertial waves, topographic waves, and a rim current). A detailed investigation of such bottom dynamics has never been performed in the southern Adriatic, even though several studies have analyzed its thermohaline properties and dense water

production rates, using either experimental [*Manca et al*., 2002; *Gačić et al*., 2002; *Cardin et al*., 2011; *Bensi et al*., 2013] or numerical approaches [*Mantziafou and Lascaratos*, 2008; *Rubino et al*., 2012; *Querin et al*., 2013].

Furthermore, recent experimental observations [*Bensi et al*., 2013] have raised new questions on the thermohaline variability in the deep layer of the SAP. In particular, temperature, salinity, and current time series collected at the E2M3A deep-ocean observatory show that the near-bottom layer was characterized by continuous, long-term temperature and salinity increase ("linear" time trends of $\sim$0.05°C/yr and $\sim$0.004 1/yr, respectively) from November 2006 until March 2012, in association with a potential density decrease. Despite the availability of extensive and continuous experimental time series, the causes of this monotonic and almost linear variability are not yet completely clear.

Thereafter, the positive trends in temperature and salinity were suddenly interrupted only by an abrupt modification of the deep layer structure due to temperature and salinity drops, which the authors related to the intrusion of very dense NAdDW. Such an episode of NAdDW formation was caused by the unusually harsh and long-lasting Bora wind event that occurred between late January and early February 2012, after a period of drought and consequent low river discharge into the northern Adriatic. That event produced a large volume of NAdDW, with record-breaking densities measured on the northern shelf (30.59 kg/m^3) [*Mihanović et al*., 2013; *Raicich et al*., 2013; *Vilibić and Mihanović*, 2013; *Janeković et al*., 2014; *Benetazzo et al*., 2014; *Carniel et al*., 2016].

In this paper, we aim to explore and understand in detail the physical processes and dense water dynamics occurring in the deep layer of the southern Adriatic Sea by merging the E2M3A in situ measurements and results provided by a numerical model of the entire Adriatic Sea with a higher-resolution downscaling focused on the southern Adriatic. We analyzed the period spanning November 2006 to December 2012 to investigate the "linear" decrease in bottom water density (in the absence of relevant dense water formation episodes) and the effect of a very intense episode of winter surface cooling (the extreme Bora episode of late January to early February 2012), which triggered the ventilation of the bottom of the SAP. In particular, we focused on the possible causes of the observed monotonic trends in bottom temperature and salinity, and we developed a hydrodynamic interpretation of the experimental data based on the numerical results.

Furthermore, we hypothesize that the continuous density decrease observed in the SAP, which was interrupted only by the intrusion of very dense water masses of northern Adriatic origin, could be one cycle of a general "saw-tooth" pattern characterized by two alternating phases. The first phase (mixing phase) corresponds to an almost linear density decrease that is induced by long-lasting mixing processes fostered by flow instabilities (e.g., mesoscale eddies). The second one (DW intrusion phase) corresponds to a sudden density increase due to the intrusion of very dense NAdDW veins that strongly depend on winter atmospheric conditions on the northern shelf (e.g., air-sea heat loss) and on NAdDW preconditioning factors (e.g., river discharge rates and thermohaline properties of the water masses advected from the southern Adriatic).

The paper is structured as follows. We describe the experimental data set and the setup of the numerical model in section 2. Section 3 is dedicated to the presentation and discussion of the results. In particular, we compare the numerical simulations with the experimental data in section 3.1, whereas in section 3.2 we introduce and describe the saw-tooth modulation of the thermohaline properties in the bottom layer of the SAP. In section 3.3, we look for evidence of the proposed cyclic alternation of the mixing and DW intrusion phases in past measurements. We summarize the paper and draw the main conclusions in section 4.

2. Materials and Methods

2.1. Experimental Data Set

The SAP has been monitored since November 2006 and currently remains under observation by means of the E2M3A deep-ocean observatory, which is located in its central part (Lat. 41°32′N, Lon. 18°05′E, Figure 1, http://nettuno.ogs.trieste.it/e2-m3a/). Several oceanographic surveys have also been performed since the eighties. *Bensi et al*. [2013, 2014] provide a detailed description of the E2M3A architecture and data set. In this study, we used the data available from November 2006 to December 2012, which were measured at five nominal sampling depths: 350, 550, 750, 1000, and 1200 m [*Cardin and Bensi*, 2014; *Cardin et al*., 2014]. The data were sampled at an hourly rate and then processed by a low-pass filter with a cutoff period of 33 h.

2.2. Numerical Model

The numerical simulations were performed using a customized version of the Massachusetts Institute of Technology general circulation model (MITgcm) [*Marshall et al*., 1997], which is a three-dimensional, finite volume, general circulation model.

2.2.1. Model Configuration

Our MITgcm setup is an upgraded version of the model described in *Querin et al*. [2013] and *Cossarini et al*. [2015]. We used a numerical grid that covered an area spanning from latitude 40°N to 46°N, featured a horizontal resolution of 1/32° and was composed of 60 unequally spaced vertical levels. We increased the vertical grid resolution below the depth of the Otranto sill (800 m) by gradually refining the grid, starting from 900 m depth and moving to the seafloor (1250 m), where the vertical spacing was reduced to 5 m. The finer vertical discretization was designed to achieve a better representation of the bathymetry of the bottom of the SAP.

To reduce the spurious diapycnal mixing (especially in the deep layer) due to the vertical z-level discretization [*Hill et al*., 2012], we adopted the second-order moment (SOM) advection scheme described by *Prather* [1986]. Furthermore, we used the Leith-Smagorinsky and KPP schemes for the horizontal and vertical parameterizations of turbulence, respectively (more details on the MITgcm parameterizations can be found at http://mitgcm.org/public/r2_manual/latest/online_documents/manual.pdf).

The adopted horizontal grid spacing (1/32°: $\sim$3.4 $\times$ 2.4 km) allows realistic simulations of the main mesoscale features of the Adriatic Sea, which are characterized by horizontal scales of approximately 5–10 km. However, to achieve a more accurate description of the processes in the SAP (i.e., full eddy resolving simulations), we also nested a 1/64° ($\sim$1.7 $\times$ 1.2 km) model of the southern Adriatic Sea into the 1/32° model of the whole Adriatic (Figure 1).

The Adriatic model receives the boundary conditions at the southern open boundary from a further MITgcm implementation of the Adriatic and Ionian Seas, which adopts the same horizontal resolution (1/32°). This latter model, called ADIOS (Adriatic Ionian system), is nested along the Sicily Strait (on the western side) and along the Cretan Passage (on the eastern side, Figure 1) into the 1/16° Mediterranean forecasting system set up in the framework of the Copernicus project (Copernicus Mediterranean Monitoring and Forecasting Centre: Copernicus-Med-MFC, http://marine.copernicus.eu). The vertical discretization adopted for the ADIOS model is the same as that of the Copernicus-Med-MFC model, except for the surface level, which was further subdivided into two equal layers to obtain a better representation of the surface processes. By doing so, the Adriatic model grid and the ADIOS model grid are exact matches along the Otranto Strait (southern open boundary of the Adriatic model) from the surface down to the depth of the Otranto sill. Therefore, there is no need to interpolate the ADIOS fields to implement the one-way nesting from the ADIOS to the Adriatic model.

The discharge rates of the main rivers flowing into the Adriatic Sea were defined taking into account the new data set presented by *Janeković et al*. [2014].

Further details on the model setup and numerical implementation are described in *Querin et al*. [2013] and *Cossarini et al*. [2015].

2.2.2. Meteorological Forcing

To drive all the numerical simulations of this study (from the ADIOS model to the SAP model), we used the meteorological forcing fields produced by the latest version of the Regional Climate Modeling system RegCM4, which was developed at the Abdus Salam International Centre for Theoretical Physics (ICTP) and described by *Giorgi et al*. [2012]. RegCM4 is a hydrostatic and terrain following sigma vertical coordinate model that has multiple physics options. Among those of interest for this study are the Biosphere-Atmosphere Transfer Scheme (BATS) [*Dickinson et al*., 1993] for the representation of land-surface processes and the cumulus convection schemes of *Grell* [1993] and *Emanuel and Živković-Rothman* [1999]. The RegCM modeling system has been used for more than two decades for a wide variety of applications, and the most up-to-date version of this community RCM is available at the following URL: http://gforge.ictp.it/gf/project/regcm/frs/.

RegCM4 was integrated over the Adriatic-Ionian basin with a horizontal grid spacing of 12 km and 23 vertical levels for the period 2006–2012. The initial and lateral meteorological boundary conditions were provided by a regional climate simulation at 50 km resolution over the Med-CORDEX domain described by A. Fantini et al. (Assessment of multiple daily precipitation statistics in ERA-Interim-driven Med-CORDEX and

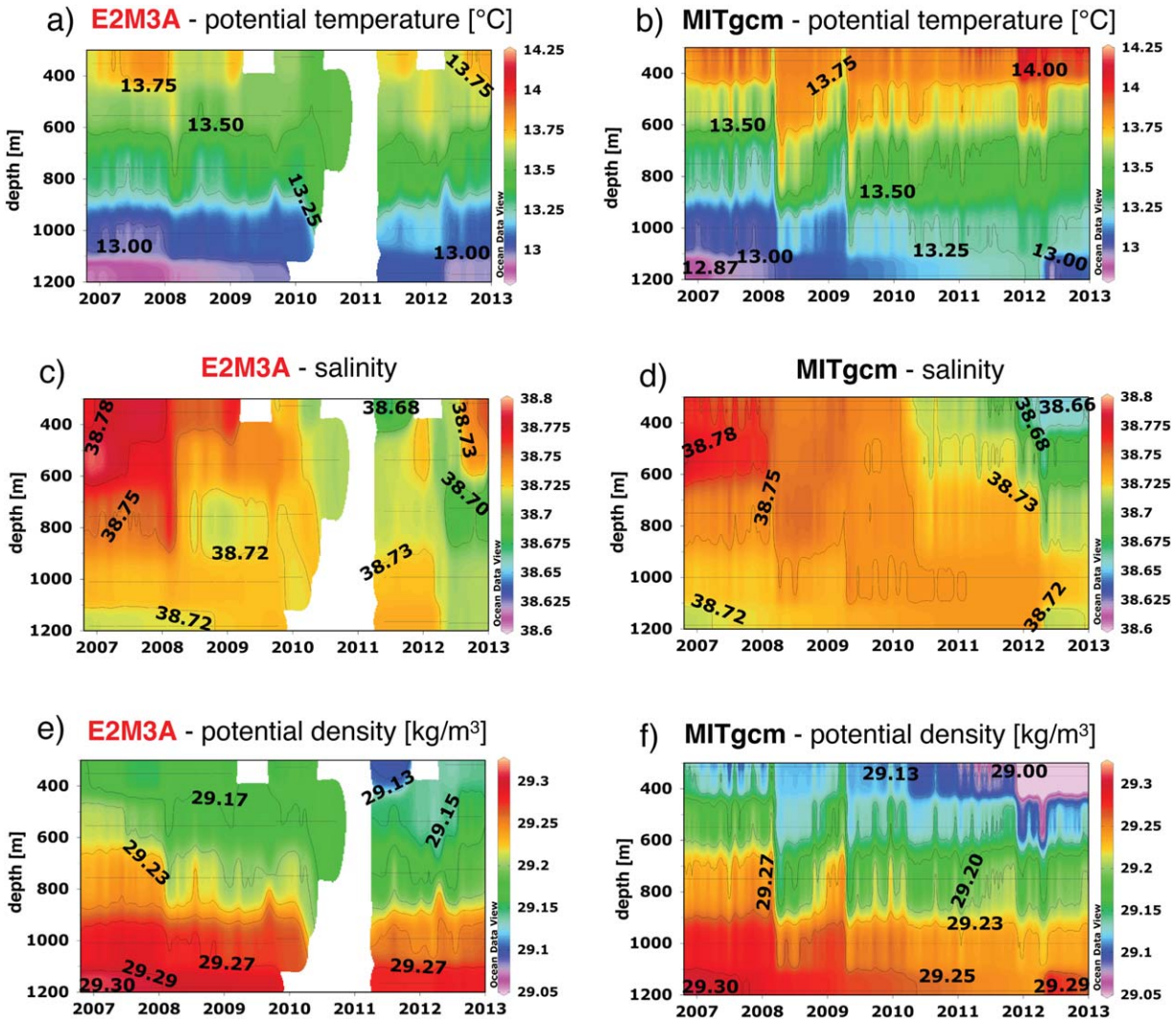

Figure 2. Comparison between the (left column) E2M3A data and (right column) model results. Hovmöller diagrams of the (a and b) potential temperature, (c and d) salinity, and (e and f) potential density. The thin horizontal lines indicate (left column) the depth of the E2M3A CTD sensors and (right column) the correspondent levels in the numerical model grid. The white areas in the plots on the left column indicate missing data.

Euro-CORDEX experiments against high resolution observations, submitted to *Climate Dynamics*, Med-CORDEX Special Issue, 2015).

Notably, a 12-km-resolution regional climate model is not able to reproduce small mesoscale atmospheric features over the Adriatic area. Therefore, a detailed simulation of the surface dynamics and DW formation processes in the northern shelf would require higher-resolution nonhydrostatic atmospheric modeling. However, since our study is focused on the bottom layer dynamics in the SAP, we basically verified that the coupled RegCM-MITgcm model produced thermohaline patterns and temporal variability that were consistent with the experimental data (see section 3.1).

2.2.3. Numerical Simulations

We ran 74-month-long simulations of the period from November 2006 to December 2012 after a spin-up run that spanned from January to October 2006. The simulated time window also covered the period during which the E2M3A measurements were missing (from the end of 2009 to the beginning of 2011), thus integrating the experimental data set.

The results and analyses presented in this paper are based on the output (daily averages) of the Adriatic and southern Adriatic models, whereas the ADIOS model was used only to provide the initial and open boundary conditions for the Adriatic model.

Table 1. Model Skill Metrics[a]

Variable	Metric	Before Tuning	After Tuning	Improvement (%)
θ (°C)	Absolute bias	1.39E-01	1.28E-01	8
	RMSE	1.72E-01	1.53E-01	11
S	Absolute bias	2.35E-02	1.49E-02	37
	RMSE	3.13E-02	1.96E-02	38
σ (kg/m^3)	Absolute bias	2.88E-02	2.77E-02	4
	RMSE	3.35E-02	3.26E-02	3

[a]Skill metrics (absolute bias and RMSE) of the model results and E2M3A data set for the simulation run without tuning the open boundary conditions ("Before Tuning," third column) and for the simulation obtained after the trial and error calibration of the open boundary condition ("After Tuning," fourth column). The first column shows the variable considered, the second the type of metric, and the fifth the improvement obtained after completing the calibration.

In the sections that follow, we assume that autumn comprises OND, winter comprises JFM, and so on.

2.2.4. Tuning of Initial and Open Boundary Thermohaline Conditions

Because our modeling effort is intended to provide a reliable interpretation of the physical processes occurring in the SAP, rather than to obtain highly accurate ($O(10^{-2})$) comparisons with experimental data, we preferred neither to condition the internal dynamics of the system during runtime nor to correct the results during the postprocessing phase. Therefore, data assimilation and bias correction algorithms (for the purpose of obtaining a better fit with the E2M3A data set) were not applied to any of the models.

Only the initial conditions for the Adriatic simulation, which were derived from the ADIOS model, were corrected in the SAP (as in *Querin et al*. [2013]) using the thermohaline profile collected at the E2M3A site in November 2006.

We reduced the misfit between the Adriatic model results and the E2M3A data set by adjusting the thermohaline properties along the southern open boundary using a trial and error procedure, whereas no updates were performed on the velocity fields. The purpose of the tuning experiments for the open boundary conditions was to achieve realistic simulations of the main dynamics captured by E2M3A, especially close to the bottom (i.e., "linear" thermohaline trends and abrupt NAdDW intrusions). We calibrated the temperature and salinity open boundary conditions by applying horizontally uniform corrections, which we varied in time and along the vertical direction, according to the improvement/worsening observed when comparing the experimental and modeled thermohaline properties at the E2M3A site. We chose the magnitude and the vertical modulation of the corrections by also relying (when available) on the vertical thermohaline profiles collected during the VECTOR (http://vector.conismamibi.it/) and SESAME (http://isramar.ocean.org.il/SESAMEMeta/) cruises, which were conducted south of the Strait of Otranto in the period 2006–2008.

Conversely, the southern Adriatic model was nested directly into the Adriatic model without further corrections to the initial conditions or open boundary conditions.

We evaluated our model performance by qualitatively and quantitatively comparing the modeled and measured temperature, salinity and potential density profiles at the E2M3A site (see section 3.1).

3. Results and Discussion

3.1. Model Performance and Comparison With Experimental Data

We checked the simulated spatial and temporal thermohaline variability in the southern Adriatic against the E2M3A data set (Figure 2).

The overall metrics of the comparison are reported in Table 1. We computed the absolute bias and RMSE between the E2M3A time series (at the five nominal depths) and the model output (at the corresponding levels of the southern Adriatic domain). Then, the overall metrics were obtained by computing the average of the five pairs of indexes (one pair for each level). Table 1 shows the metrics calculated before and after the tuning procedure, which was performed along the southern open boundary of the model (section 2.2.4). We obtained a general improvement in model performance for the temperature and salinity, with a consequent improvement for density.

Moreover, the calibration was also undertaken to enhance the consistency of the simulated thermohaline variability in depth and time against the variability observed by E2M3A (Figure 2). In particular, after the calibration, the model correctly simulated several oceanographic processes, including the pronounced (down to ~800 m depth) deep convection of February 2008 (which was absent in winter 2007) and the continuous

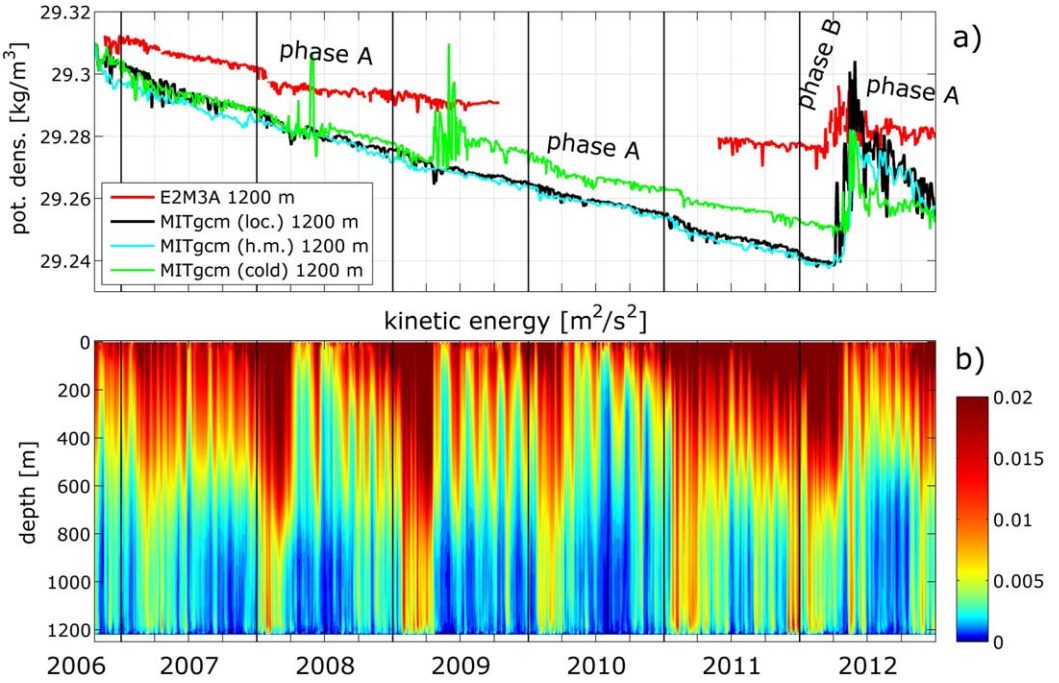

Figure 3. (a) Comparison between the daily averaged E2M3A data (red line) and model results (black—local value, blue—layer horizontal mean, and green—cold boundary conditions experiment) at 1200 m depth. (b) Hovmöller diagrams of modeled kinetic energy averaged over an area of 70 × 70 km, centered on the E2M3A position. The color bar in Figure 3b is stretched to highlight the processes that occur in the intermediate and bottom layers of the SAP.

and monotonic density decrease below 1000 m depth until March 2012 (Figures 2e and 2f). The numerical simulations also reproduced the general salinity decrease over time in the layer spanning depths from ∼300 to ∼800 m (Figures 2c and 2d). Conversely, the model tended to overrate the temperature (Figures 2a and 2b). It also overestimated the deep convection episode of winter 2009 and missed the intrusion of relatively salty water masses between 300 and 600 m depth after mid 2012 (Figures 2c and 2d).

If we focus on the bottom layer of the SAP, which was monitored by conductivity-temperature sensors located at 1200 m depth (Figure 3a, red line), we can observe a clear decreasing trend in potential density from November 2006, when measurements commenced, to March 2012. This almost linear decrease (observed 0.007 kg/m^3/yr) was interrupted only by a sudden intrusion of very cold and relatively fresh (overall very dense) water of northern Adriatic origin [*Bensi et al.*, 2013]. Then, in the late spring of 2012, the decrease in density began again.

For the sake of clarity, in this paper, we define the density decrease period as "phase A" and the sudden density increase (0.02 kg/m^3 observed over a few weeks) as "phase B." A comparison between the data (Figure 3a, red line) and model results (Figure 3a, black line) shows that the model tended to overestimate the density decrease (phase A). The monotonic (almost linear) trend is qualitatively well reproduced throughout the simulated period, although the modeled decrease in potential density is almost twice as large as the measured one. Regarding the sudden density rise (phase B), the timing of the DW arrival (first pulses recorded in early March 2012) and the highest density recorded (29.297 kg/m^3, data; 29.303 kg/m^3, model) were simulated satisfactorily, even if the modeled NAdDW appeared in the bottom of the SAP after a delay of a few days.

The blue line in Figure 3a represents the density horizontally averaged over the whole layer at 1200 m depth, and the black line refers "exactly" (i.e., the nearest grid element) to the E2M3A position, which is located close to the center of that area. The fact that the density at the E2M3A position is almost always slightly higher than the average of the whole layer is evidence of the dome-like structure of the isopycnals in the bottom of the SAP (see section 3.2.1).

Additional details on the comparison between the model results and experimental data (potential temperature, salinity, and potential density) at several locations in the northern Adriatic are presented in

Table 2. Thermohaline Properties in the Winter/Spring of 2012[a]

		Depth (m)		θ (°C)			S			σ (kg/m^3)		
Station	Date in 2012	Data	Model	Data	Model	M-D	Data	Model	M-D	Data	Model	M-D
TS (Gulf of Trieste)	15 Feb	18.0	19.7	4.24	3.81	−0.42	38.56	38.05	−0.51	30.59	30.23	−0.36
AA (Acqua Alta)	11 Feb	13.0	11.6	6.35	5.63	−0.72	38.60	38.15	−0.45	30.35	30.09	−0.26
PC (Pag Channel)	29 Mar	101.1	92.1	9.36	8.19	−1.18	38.77	38.89	0.12	30.02	30.30	0.28
TL (Telašćica)	29 Feb	34.3	34.2	9.15	11.54	2.39	38.68	38.71	0.02	29.98	29.56	−0.42
AR (Argo 1900848)	4 Apr	96.0	92.1	9.54	9.18	−0.36	38.64	38.80	0.16	29.88	30.07	0.19
DR (Drage)	28 Feb	29.0	29.0	10.28	10.58	0.29	38.72	38.73	0.01	29.81	29.76	−0.05
JP (Jabuka Pit)	27 Apr	266.0	247.0	10.00	9.73	−0.28	38.63	38.72	0.08	29.79	29.91	0.12
P2 (Palagruža Sill)	16 Mar	130.0	135.6	10.58	11.24	0.66	38.64	38.50	−0.14	29.69	29.46	−0.23
P1 (Palagruža Sill)	26 Apr	171.0	177.0	10.93	10.42	−0.51	38.70	38.68	−0.02	29.67	29.75	0.08
ZD (Zadar)	27 Mar	30.0	29.0	11.53	9.28	−2.25	38.83	38.79	−0.03	29.66	30.04	0.38
MS (Maslenica)	29 Mar	24.5	24.2	6.95	8.18	1.23	37.79	38.77	0.98	29.63	30.21	0.58
ST (Split Channel)	21 Feb	47.5	45.8	10.94	9.08	−1.86	38.56	38.45	−0.11	29.57	29.81	0.24
BL (Blitvenica)	28 Feb	196.5	192.7	12.00	11.70	−0.29	38.64	38.63	−0.01	29.43	29.47	0.04
HV (Hvar)	21 Feb	72.5	74.5	12.23	12.15	−0.08	38.64	38.63	−0.01	29.38	29.38	0.00

[a]Comparison between the model results and the experimental data reported in *Mihanović et al*. [2013, Figure 1 and Table 1]: thermohaline properties measured at 14 stations in the Adriatic Sea [*Mihanović et al*., 2013, Figure 1] and the corresponding model output (daily averaged results computed for the same day, at the closest grid point in the model domain). The first four columns show the station name, sampling date, and real and modeled sampling depths. The other columns show the measured, modeled, and bias (model-data) values of the temperature, salinity, and potential density.

Table 2. In this case, the experimental data refer to the data set reported in *Mihanović et al*. [2013, Figure 1 and Table 1] for the exceptional dense water production event that occurred in winter 2012. Overall, the agreement is satisfactory, with absolute biases and RMSEs (for temperature, salinity and density) of 0.89°C, 0.19, 0.23 kg/m^3 and 1.16°C, 0.33, 0.28 kg/m^3, respectively. Table 2 shows that the data measured at the most significant open sea stations (Palagruža sill, Jabuka pit, and Argo float) were simulated correctly by the model, but remarkable differences can be found, especially along the Croatian coast. In that area, complex morphologic, hydrologic, and bathymetric features (with many islands, rivers, and narrow channels) induce small-scale features and pronounced thermohaline variability, which cannot be fully resolved by the model.

In the late winter of 2012, the simulated total volume of water denser than 29.5 kg/m^3 was 4357 km^3. Our results are in good agreement with the estimates made by *Mihanović et al*. [2013] (i.e., 4250 km^3).

3.2. Interpretation of Results: The Saw-Tooth Modulation of the Bottom Layer Thermohaline Variability

3.2.1. Phase A: Long-Lasting Density Decrease

When seeking an explanation for the monotonic potential density decrease in the bottom layer of the SAP (phase A), we can easily exclude some possible causes. First, we can rule out any spurious drift in the experimental data set because the sensors were checked and calibrated before and after each deployment. Moreover, the time series were compared with CTD data collected during several oceanographic surveys in the area [*Bensi et al*., 2013]. We can also exclude any possible thermal or chemical contributions from external sources (e.g., submerged vents or volcanoes) because the model reproduced the bottom dynamics without considering any kind of external source. Lastly, the thermohaline trend cannot be ascribed to the open-ocean convection in the southern Adriatic. Indeed, open-ocean convection is a sporadic process that cannot produce linear trends, it is very limited in time (up to a few days) and, in the last two decades, it has never involved the layer of the SAP below 1000 m depth. Hence, we hypothesize that the slow and continuous mixing process induced by the almost permanent, geostrophic cyclonic circulation in the southern Adriatic (Figures 4b–4d) is the primary driver of the "linear" time trend in the bottom temperature and salinity. Indeed, a generic water parcel in the center of the pit is surrounded by lighter water both at the top (due to the water column stratification) and all around (due to the doming of the isopycnals, Figure 4b). In the idealized case of a stable, inviscid and permanent geostrophic flow, the thermohaline properties of the system are not supposed to change over time. On the contrary, real geostrophic flows are prone to instabilities and growing perturbations. In particular, model results have shown that larger-scale structures (i.e., eddies and meanders) efficiently transport light water from the top and, most important, from the periphery to the center of the gyre, whereas smaller-scale turbulence mixes the advected water masses with the local (denser)

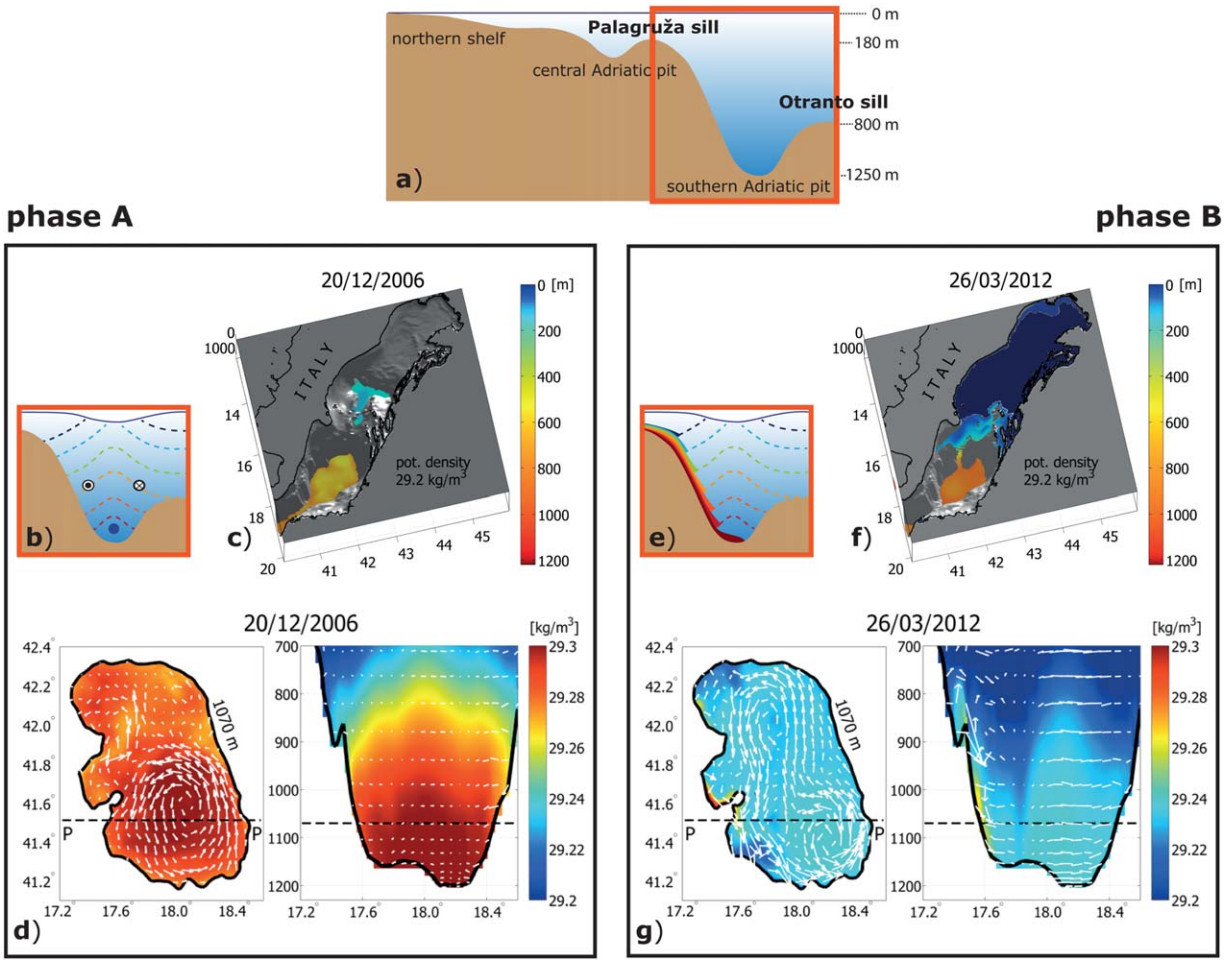

Figure 4. (a) Idealized vertical section along the Adriatic Sea, and a theoretical/numerical description of phase A (left box) and phase B (right box): (b and e) idealized sketches of the SAP and (c, d, f, and g) model results (daily averages of the model output on two selected days). (b) An idealized representation of the cyclonic circulation in a stratified southern Adriatic Sea, with the surface depression in the middle of the gyre and the doming of the isopycnals (the line curvature is magnified for the sake of clarity). A generic water parcel located in the bottom of the SAP is indicated by the blue dot. (e) The cascading of the NAdDW. (c and f) A basin-scale, three-dimensional view of the potential isopycnals (the color of the isosurfaces is proportional to the depth). (d and g) The horizontal and vertical sections of potential density in the SAP. White vectors show the (left) horizontal and (right) zonal/vertical velocity components. The vertical velocity component is magnified for the sake of clarity.

water masses (see the supporting information for more details). This process is analogous to the turbulent energy cascade in fluid dynamics. As a result, the thermohaline properties tend to slowly homogenize.

The hydrodynamic features simulated for the SAP case study are consistent with those described by *Spall* [2003, 2004] for an idealized marginal sea, where the heat loss in the interior is balanced by lateral eddy fluxes originating from a warm peripheral boundary current. The backdrop of the present study is slightly different: we built our numerical simulations on a realistic domain with realistic forcings, and, in such a context, flow instabilities arise from a permanent geostrophic rim current affecting the relatively deep oceanic pit. In both situations, advection plays a crucial role in varying the thermohaline properties of the basin, whereas diffusion has a minor effect.

We highlight the relative contribution of advection and diffusion to the total simulated potential temperature trend in the deep layer of the SAP in Figure 5. The temperature tendency (T_{tend} [°C/s]) computed by the model is comprised of the following terms:

$$T_{tend} = ADV_x + ADV_y + ADV_z + DF_x + DF_y + DF_z \quad (1)$$

where ADV_x, ADV_y, and ADV_z and DF_x, DF_y, and DF_z are the tendencies due to advection and diffusion in the zonal, meridional, and vertical directions, respectively. When using the KPP parameterization, vertical

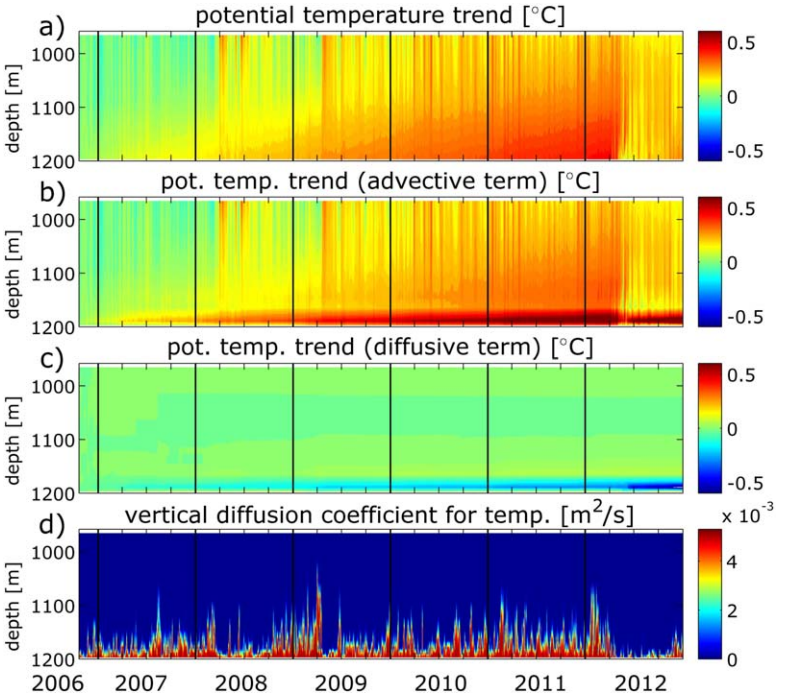

Figure 5. Modeled bottom layer properties at the E2M3A site. Hovmöller diagrams of the simulated potential temperature trend ((a) total, (b) separate contribution due to advection, and (c) diffusion) and of the vertical diffusion coefficient for temperature.

diffusivity is computed via an implicit scheme; hence, the term DF_z comprises the implicit vertical diffusivity (the explicit term is null) and the contribution due to KPP. Notably, the contribution to the total budget due to surface heat flux and shortwave penetrative radiation is negligible in the deep layers. The time-integrated tendency gives the temperature trends (°C) depicted in Figures 5a–5c for the total, advective, and diffusive terms, respectively. Below 950 m depth, the temperature trend (which increases monotonically below 1100 m) is almost totally due to advection, whereas diffusion plays a significant role in the deepest 20–30 m. Figure 5d indeed shows that the vertical diffusion coefficient is significant only close to the seafloor, due to bottom friction. In this specific case study, diffusion compensates the temperature excess due to advection. Contrary to the vertical diffusion and accordingly to the present model setup (horizontal eddy diffusivity set to 10^{-2} m^2/s), the horizontal diffusion is negligible throughout the whole domain (not shown).

Similar to *Spall* [2004], where the exchange of heat and momentum in the idealized marginal sea is carried by horizontal eddies and there is no mean baroclinic overturning circulation, the water mass transformation in the bottom of the SAP is most likely driven by horizontal flow instabilities (see the supporting information) and not by vertical processes (convection and/or vertical diffusion and/or baroclinic overturning circulation).

In the previous sections, we referred to the "linear" time trends in the measured and modeled thermohaline properties at the bottom. Actually, the slopes of the density trends display some discontinuities; for example, the measured density time series shows a small falloff in the winter of 2008, whereas the model results are affected by a slight intensification of mixing not only in the winter of 2008, but also in the winter of 2009, 2011, and 2012. Overall, the correlation coefficient between the observed and modeled bottom density trends is 0.90. Figure 3b presents the Howmöller diagram of the kinetic energy averaged over an area of 70 × 70 km centered on the E2M3A position. Figure 3 hints that the intensifications observed in the decreasing density trends (Figure 3a) must be ascribed to a general increase in the kinetic energy (Figure 3b) and to an enhanced cyclonic circulation throughout the water column (from the surface to the bottom) due to the deep convection. Indeed, the bottom model density trend is anticorrelated with the time integral of the bottom kinetic energy (correlation coefficient: −0.77); the density decreased more rapidly as the kinetic energy increased.

We must also note that the mixing at the bottom is only indirectly related to the deep convection (which has never reached the bottom of the SAP); the latter enhances the cyclonic circulation in the basin

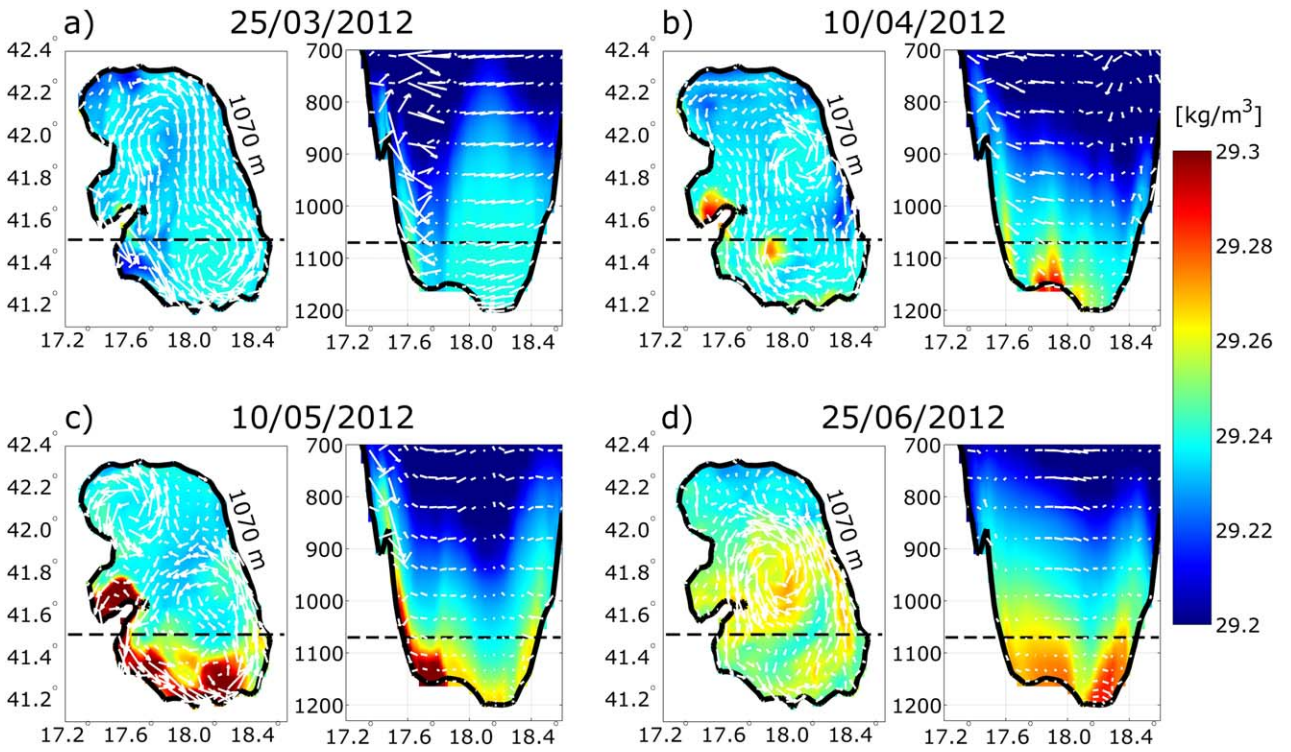

Figure 6. Phase B: horizontal and vertical sections of potential density and velocity in the SAP, as described in Figures 4d and 4g (daily averages on four selected days in the period March–June 2012). Each plot shows the horizontal section of potential density in the southern Adriatic at a depth of 1070 m and a vertical section at the same latitude as the E2M3A (section P-P in Figure 1), from a depth of 700 m to the bottom. The white vectors show (left) the horizontal and (right) the zonal/vertical velocity components. The vertical velocity component is magnified for the sake of clarity.

(intensification of the rim current produced after the convective overturning phase [*Send and Marshall*, 1995]), from which the instabilities that cause the former originate.

3.2.2. Phase B: Sudden Density Increase

The sudden density increase observed in the late winter of 2012 (phase B) was induced by the exceptional NAdDW formation event of late January to early February 2012. This large amount of very dense water was finally able to sink and reach the bottom of the SAP a little more than a month after its generation on the northern shelf. Figure 4 shows an idealized sketch (plot e) and the simulated NAdDW vein sinking in the SAP along the shelf break and Bari canyon system (plot f and g). Contrary to the mixing phase (phase A), which lasted from late 2006 to early 2012 and can be considered to be the typical hydrodynamic condition of the deep layer of the SAP, phase B represents an episodic perturbation of the system. The bottom flow of the NAdDW flushed the SAP, replaced the local water masses and ventilated the deep layer very efficiently. Figure 4g shows one among several dense ($>$29.27 kg/m^3) and narrow NAdDW veins sinking toward the SAP in the second half of March.

Figure 6 highlights the complexity of the NAdDW cascading phase (also see the supporting information) reproduced by the numerical model. More than a month after the Bora event (late March 2012), isolated and relatively dense ($\sim$29.25 kg/m^3) pulses of NAdDW, originated on the shelf, sank almost to the bottom of the SAP (plot a). The NAdDW flow became steadier (less pulsating) and intense two months after the end of the Bora event (April 2012), when the large volume of dense water ($>$ 29.27 kg/m^3) that had formed on the shelf massively flowed toward the deepest layers (plot b). After reaching the southern Adriatic, the NAdDW was embedded in the local cyclonic circulation. Hence, the sinking process was not purely vertical; the NAdDW flowing in the SAP followed a spiral-shaped trajectory, with both vertical (downward) and horizontal (cyclonic) components of velocity (Figures 6b and 6c). The cascading of the NAdDW continued in the early spring (plot c) and slowly decreased until it finally ceased in June (plot d), when the thermohaline properties almost reached the same values that had been observed three years earlier (Figure 3a). The experimental data and model results then show that the slow homogenization of the deep layer (phase A) associated with the stable cyclonic circulation started again (Figure 3a).

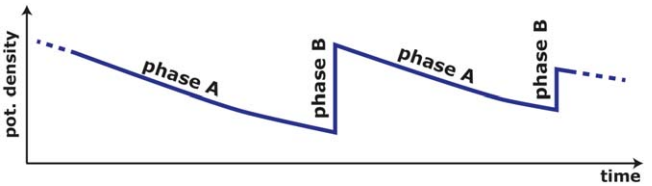

Figure 7. Saw-tooth modulation over time for the long-lasting mixing process (potential density decrease, phase A) and sudden NAdDW intrusion episodes (potential density increase, phase B).

Model simulations have also provided useful basin-scale information on DW volumes and discharge rates. The simulated total volume of water denser than 29.5 kg/m^3 (4357 km^3) produced in the winter of 2012 was more than an order of magnitude larger than the DW volume produced in 2008 (342 km^3), which can be considered in terms of surface heat fluxes and from a climatological point of view to have been a year characterized by average winter conditions [*Bensi et al*., 2013; *Querin et al*., 2013].

Exceptional NAdDW volumes entail exceptional NAdDW flow rates; in the winter and early spring of 2012, the southeastward flow of water denser than 29.25 kg/m^3 across a vertical section on the northern shelf (section S-S, Figure 1) was, on average, approximately 0.5 Sv, with peaks up to 2 Sv. The average flow during the same period in 2008 was almost 5 times smaller [*Querin et al*., 2013].

3.2.3. Cyclic Alternation of Phase A and Phase B

If we assume that the mixing phase lasts for a much longer time (i.e., many years without NAdDW intrusions) and if we neglect the thermohaline variability in the layer above 1000 m depth, then the deep layer of the SAP would tend to asymptotically reach an equilibrium value (complete homogenization). Clearly, this is not the case; NAdDW intrusions occasionally perturb the system, and the general circulation above the level of the Otranto sill (800 m) affects the layer above 1000 m depth (due to local mixing and entrainment).

In light of these considerations, we hypothesize a (nonperiodic) cyclic, "saw-tooth" modulation of phase A and phase B over time (Figure 7). The length and steepness of phase A and the return period and magnitude of phase B depend on the local meteorological and oceanographic conditions.

In particular, the occurrence of phase B is related to the difference in density between the NAdDW vein and the ambient water inside the SAP; the former must be dense enough to sink and flush the latter from the bottom of the SAP. NAdDW density (and volume) depends on several factors, namely the intensity of winter surface fluxes (cooling and evaporation, which are strongly related to wind, and precipitation) and the influence of lateral forcings (river discharge rates and the thermohaline properties of the water masses coming from the southern Adriatic). Hence, a cold, dry, and windy winter season is a necessary but not sufficient condition for the occurrence of phase B, which should be related also to the thermohaline properties of the entire Adriatic Sea (precondition for the NAdDW formation).

Phase B usually lasts for a few months: from the arrival of the first DW pulses (late winter/spring) to the depletion of the NAdDW vein (spring/early summer). On the other hand, we cannot specify a typical timespan for phase A due to the sporadic nature of phase B. In the present case study, phase A, which lasted for more than 5 years (at least), was interrupted only by the very exceptional NAdDW formation event of winter 2012.

We corroborated our hypothesis by also performing a further idealized experiment that featured a colder boundary condition at the northern and western sides of the southern Adriatic model domain ("cold" experiment in Figure 3a). We simulated denser water masses coming from the northern shelf by decreasing the temperature at the boundaries of 0.5°C. The effects of this change are shown by the green line in Figure 3a; in spring 2008, the decreasing trend of potential density is interrupted by a few high-density peaks followed by a small density increase ($\sim$0.003 kg/m^3). The subsequent linear trend is interrupted again in spring 2009, with a much more remarkable signal of density increase ($>$0.01 kg/m^3). Afterward, NAdDW production (both in 2010 and 2011) is unable to interrupt the density decrease until the 2012 event. In conclusion, although with different periodicities and amplitudes of the density increase, the cyclic alternation of phase A and B seems to be a peculiar feature of the bottom layer of the SAP.

3.3. Evidence of the Hypothesized Saw-Tooth Modulation in Past Measurements

The high-temporal-resolution experimental data set analyzed in the previous sections has proved to be a useful tool to detect short-term processes such as deep convection episodes in the open sea or dense water overflows (e.g., cascading) in the bottom layer of the SAP. In particular, the thermohaline variability

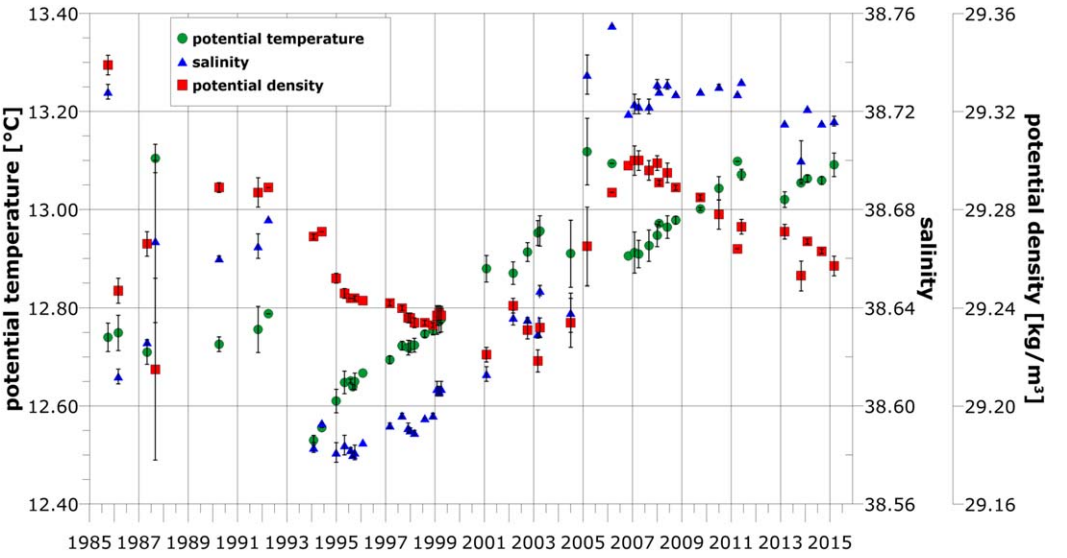

Figure 8. Time series of the potential temperature, salinity, and potential density obtained by computing the spatial averages in the central SAP region for all the available CTD data below 1000 m depth collected during the oceanographic cruises performed in the period 1985–2014.

measured by the deepest sensors (1200 m depth) at E2M3A during 7 years revealed one cycle of the supposed saw-tooth modulation of the bottom thermohaline properties, which we presented in section 3.2. Here, to find evidence of further comparable signals in the past, we analyze the data collected during several oceanographic campaigns carried out almost regularly in the SAP in the last three decades, following the methodology described by *Cardin et al.* [2011]. Contrary to the local E2M3A data set, cruise CTD data are characterized by wider horizontal coverage and very fine vertical resolution, even though the sampling frequencies are inherently much lower. Therefore, local and short-lived processes cannot always be sampled effectively. Being aware of this limitation, available CTD data spanning 1985–2014 have been used to analyze the thermohaline variability in the layer extending from 1000 m depth to the seafloor. Figure 8 shows the values obtained by performing spatial averages in the central SAP region (between latitudes 41.25°N–42.25°N and longitudes 17.25°E–18.25°E) of all the available cruise data below 1000 m depth (see *Cardin et al.* [2011], for further details). The thermohaline variability in this part of the water column is mainly influenced by the advection of NAdDW, which can reach different neutrally buoyant depths depending on the density difference between the NAdDW and the ambient water in the SAP. Specifically, extremely dense NAdDW is due to the very low temperature and very high salinity in the northern Adriatic. The latter can be ascribed to strong evaporation (induced by winds), low river discharges and to the large-scale circulation changes in the Ionian Sea such as northern Ionian Gyre reversals, which cause the redistribution of salt in the eastern Mediterranean Sea [*Gačić et al.*, 2010]. Furthermore, a 30-year-long time series of temperature and salinity can also be used to highlight the interannual and the decadal variabilities, which are intimately linked to large-scale variability (e.g., Adriatic-Ionian interactions) as well as to local climatic conditions (e.g., open-sea convection episodes) [*Vilibić and Orlić*, 2002; *Cardin and Gačić*, 2003; *Gačić et al.*, 2010]. The temperature and salinity time series in the SAP (Figure 8) show two abrupt thermohaline shifts in 1993 and 2006, which could be ascribed to past saw-tooth cycles. Interestingly, both events roughly coincided with the final period of a cyclonic phase of the northern Ionian Gyre, during which the Adriatic Sea experienced a progressive salinity increase.

The first event, which was observed in 1993, can be associated with the severe autumns/winters recorded in 1991/1992 and 1992/1993. During the former, the convection in the SAP that mixed the water column down to 800 m depth was primarily due to the remarkable heat loss in the southern Adriatic, whereas in 1993 the production of dense water was mainly driven by the harsh winter conditions over the northern shelf [*Cardin and Gačić*, 2003]. The resulting dense water mass (very cold but relatively fresh due to the concurrent inflow of low-salinity water from the Otranto Strait [*Cardin et al.*, 2011]) reached the bottom of the SAP and caused abrupt decreases in the temperature and salinity (almost 0.30°C and 0.1, respectively).

The second event (2006) was characterized by a smaller temperature decrease (0.20°C) associated with a salinity increase; the air-sea heat budget computed over the northern Adriatic Sea [*Bensi et al*., 2013] shows a remarkable heat loss during autumn/winter 2004/2005 and 2005/2006, which certainly triggered the formation of very dense water masses. As a result, the bottom water in the SAP reached a density of $\sim$29.31 kg/m^3 at the end of 2006, as shown in Figures 3a and 8.

Last, Figure 8 shows that the exceptional NAdDW formation event in 2012 is pinpointed by the less remarkable signal in the thermohaline time series. This apparent inconsistency might be ascribed to the coarse sampling frequency in time (with no data in 2012) and to the fact that the values in the figure originate from vertical averages within a 200-m-thick layer. The averaging process probably smoothed the signal of the very dense bottom water, which remained trapped in the deepest layer of the SAP. In fact, the E2M3A data (see Figure 3a and *Bensi et al*. [2013]) reveal two interesting aspects; on the one hand, the 2012 NAdDW intrusion event influenced the 1200 m time series more than the 1000 m one, and on the other hand, this abrupt temperature and salinity decrease faded away quite quickly (less than 1 year), confirming that the mixing processes can be very effective in the SAP.

4. Summary and Conclusions

In this study, we investigated the dynamics of the bottom layer of the SAP by merging the information obtained from an experimental data set (E2M3A deep-ocean observatory) and the results of two numerical models (the Adriatic and southern Adriatic Sea implementations of the MITgcm model).

The proposed integrated experimental-modeling approach has enabled a better understanding of the dynamics in the study area. In particular, the 3-D numerical simulations provided a basin-scale interpretation of the oceanographic features highlighted by the experimental findings, namely the slow and constant density decrease (phase A) that was abruptly interrupted by the intrusion of very dense water masses originated on the shelf during the winter of 2012 (phase B). In general, we describe the bottom of the SAP as a system that is characterized by these two alternating phases.

We have shown that the long-lasting (more than 5 years: November 2006 to March 2012) "linear" density decrease (related to a temperature and salinity increase—phase A) is due to local mixing that is fostered by flow instabilities and mesoscale turbulence, which originates from the large-scale cyclonic circulation. During that phase, the bottom layer (below 1000 m depth) is not efficiently ventilated, and the bottom of the SAP behaves like a "separate" system. Moreover, as already illustrated by *Spall* [2003, 2004] for idealized case studies, we have described the homogenization of the vertically stratified thermohaline properties in terms of horizontal flow instabilities, while we did not use the one-dimensional (vertical) eddy diffusivity coefficients to parameterize the mixing processes, which are intrinsically three-dimensional. Last, we have shown that the thermohaline trends in the deepest layer (below 1000 m) are mainly driven by advection, whereas the diffusion is considerable only very close to the seafloor (20–30 m), due to bottom friction (Figure 5).

Conversely, the sudden density increase (phase B) is associated with a drastic water mass renewal, which is induced by the formation and spreading of large amounts of NAdDW that is sufficiently dense to sink to the bottom of the SAP.

Those two phases alternate in time and induce a "saw-tooth" modulation of the thermohaline variability (Figure 7). In normal and unperturbed conditions, bottom water tends naturally to homogenize until a sufficiently dense NAdDW vein flushes the bottom of the SAP. Under this assumption, the intense ventilation of the bottom layer of the SAP depends on the "return period" of exceptionally cold, dry, and windy winters in the northern Adriatic and on the thermohaline properties of the entire basin (the densities of the bottom of the SAP and the currents flowing from the southern Adriatic to the northern shelf).

We hypothesize that these deep layer dynamics could be a typical feature of other DW formation sites in the world ocean formed by a shallow shelf ending in a pit and characterized by a persistent circulation pattern associated with sporadic intrusions of very dense water masses that originate on shelves. For example, similar behavior has been recorded in Baltic Sea fjords [*Stigebrandt and Aure*, 1989] as well as in deep subbasins of the central and northern Aegean Sea (a DW formation area of the eastern Mediterranean Sea). In fact, an analysis by *Zervakis et al*. [2003] provided estimates of vertical eddy diffusivities and turbulent buoyancy fluxes that explained an observed North Aegean deep layer density decrease during stagnation

periods following intense dense water formation events. A more recent work by *Tsabaris et al*. [2014] and new analyses by V. Zervakis (personal communication, 2014) suggest that the decreasing density phase can level off if the timespan between two consecutive dense-water formation events is very long; North Aegean measurements from the period 1994–2010 suggest that if stagnation periods last long enough for the stratification between intermediate and deep layers to be eroded, steady state conditions emerge and convective/upwelling and turbulent vertical fluxes are minimized.

Acknowledgments

This research was funded by the Italian VECTOR (sub-attività 6.4.2: Modellazione flussi di C a scala temporale breve (nord Adriatico) ed export dalla piattaforma) and RITMARE (La ricerca italiana per il mare, Italian Ministry of Education, University and Research) projects. This study was also supported by the European Union Seventh Framework Programme (FP7/2007-2013) under grant agreement 312463, FixO^3 (Fixed point Open Ocean Observatory network, http://www.fixo3.eu/). The authors thank Dario Giaiotti (ARPA FVG-CRMA) for his comments on this study. We are grateful to Valentina Mosetti and Gianpiero Cossarini (OGS) for their support and to Renzo Mosetti, Alessandro Crise, Paolo Lazzari (OGS), and Vassilis Zervakis (Univ. of the Aegean) for their valuable discussions. E2M3A experimental data are available at http://nettuno.ogs.trieste.it/e2-m3a/CTD.html#. The time series for the period 1985–2015 reported in Figure 8 are available at http://nodc.ogs.trieste.it/nodc/. Please contact S. Querin (squerin@inogs.it) for model output data and analyses.

References

Benetazzo, A., A. Bergamasco, D. Bonaldo, F. M. Falcieri, M. Sclavo, L. Langone, and S. Carniel (2014), Response of the Adriatic Sea to an intense cold air outbreak: Dense water dynamics and wave-induced transport, *Prog. Oceanogr.*, *128*, 115–138, doi:10.1016/j.pocean.2014.08.015.

Bensi, M., V. Cardin, A. Rubino, G. Notarstefano, and P. M. Poulain (2013), Effects of winter convection on the deep layer of the Southern Adriatic Sea in 2012, *J. Geophys. Res. Oceans*, *118*, 6064–6075, doi:10.1002/2013JC009432.

Bensi, M., V. Cardin, and A. Rubino (2014), Thermohaline variability and mesoscale dynamics observed at the deep-ocean observatory E2M3A in the Southern Adriatic Sea, in *The Mediterranean Sea: Temporal Variability and Spatial Patterns*, edited by G. L. E. Borzelli et al., pp. 139–155, John Wiley, Oxford, U. K., doi:10.1002/9781118847572.ch9.

Cardin, V., and M. Bensi (2014), E2M3A-2006-2010-time-series-SouthAdriatic, Ist. Naz. di Oceanogr. e di Geofis. Sperimentale, Div. of Oceanogr., 100 files, doi:10.6092/36728450-4296-4e6a-967d-d5b6da55f306. [Available at http://nodc.ogs.trieste.it/.]

Cardin, V., and M. Gačić (2003), Long-term heat flux variability and winter convection in the Adriatic Sea, *J. Geophys. Res.*, *108*(C9), 8103, doi:10.1029/2002JC001645.

Cardin, V., M. Bensi, and M. Pacciaroni (2011), Variability of water mass properties in the last two decades in the South Adriatic Sea with emphasis on the period 2006–2009, *Cont. Shelf Res.*, *31*, 951–965, doi:10.1016/j.csr.2011.03.002.

Cardin, V., M. Bensi, G. Siena, and L. Ursella, (2014), E2M3A-2011-2013-time-series-SouthAdriatic, Ist. Naz. di Oceanogr. e di Geofis. Sperimentale, Div. of Oceanogr., doi:10.6092/84cb588d-97e5-4c64-91bb-ba6109dfa530, 67 files. [Available at http://nodc.ogs.trieste.it/.]

Carniel, S., D. Bonaldo, A. Benetazzo, A. Bergamasco, A. Boldrin, F. M. Falcieri, M. Sclavo, F. Trincardi, and L. Langone (2016), Off-shelf fluxes across the southern Adriatic margin: Factors controlling dense-water-driven transport phenomena, *Mar. Geol.*, *375*, 44–63, doi:10.1016/j.margeo.2015.08.016.

Cossarini, G., S. Querin, and C. Solidoro (2015), The continental shelf carbon pump in the northern Adriatic Sea (Mediterranean Sea): Influence of wintertime variability, *Ecol. Model.*, *314*, 118–134, doi:10.1016/j.ecolmodel.2015.07.024.

Dickinson, R., A. Henderson-Sellers, and P. Kennedy (1993), Biosphere-Atmosphere Transfer Scheme (BATS) version 1 as coupled to the NCAR community climate model, *NCAR Tech. Note NCAR/TN-387+ STR*, NCAR, Boulder, Colo.

Emanuel, K. A., and M. Živković-Rothman (1999), Development and evaluation of a convection scheme for use in climate models, *J. Atmos. Sci.*, *56*, 1766–1782, doi:10.1175/1520-0469(1999)056 < 1766:DAEOAC>2.0.CO;2.

Gačić, M., G. Civitarese, S. Miserocchi, V. Cardin, A. Crise, and E. Mauri (2002), The open-ocean convection in the Southern Adriatic: A controlling mechanism of the spring phytoplankton bloom, *Cont. Shelf Res.*, *22*, 1897–1908, doi:10.1016/S0278-4343(02)00050-X.

Gačić, M., G. L. E. Borzelli, G. Civitarese, V. Cardin, and S. Yari (2010), Can internal processes sustain reversals of the ocean upper circulation? The Ionian Sea example, *Geophys. Res. Lett.*, *37*, L09608, doi:10.1029/2010GL043216.

Giorgi, F., et al. (2012), RegCM4: Model description and preliminary tests over multiple CORDEX domains, *Clim. Res.*, *52*, 7–29, doi:10.3354/cr01018.

Grell, G. A. (1993), Prognostic evaluation of assumptions used by cumulus parameterizations, *Mon. Weather Rev.*, *121*, 764–787, doi:10.1175/1520-0493(1993)121 < 0764:PEOAUB>2.0.CO;2.

Hainbucher, D., A. Rubino, and B. Klein (2006), Water mass characteristics in the deep layers of the western Ionian Basin observed during May 2003, *Geophys. Res. Lett.*, *33*, L05608, doi:10.1029/2005GL025318.

Hill, C., D. Ferreira, J.-M. Campin, J. Marshall, R. Abernathey, and N. Barrier (2012), Controlling spurious diapycnal mixing in eddy-resolving height-coordinate ocean models—Insights from virtual deliberate tracer release experiments, *Ocean Modell.*, *45–46*, 14–26, doi:10.1016/j.ocemod.2011.12.001.

Holtermann, P. L., H. Burchard, U. Gräwe, K. Klingbeil, and L. Umlauf (2014), Deep-water dynamics and boundary mixing in a nontidal stratified basin: A modeling study of the Baltic Sea, *J. Geophys. Res. Oceans*, *119*, 1465–1487, doi:10.1002/2013JC009483.

Janeković, I., H. Mihanović, I. Vilibić, and M. Tudor (2014), Extreme cooling and dense water formation estimates in open and coastal regions of the Adriatic Sea during the winter of 2012, *J. Geophys. Res. Oceans*, *119*, 3200–3218, doi:10.1002/2014JC009865.

Malanotte-Rizzoli, P. (1991), The Northern Adriatic Sea as a prototype of convection and water mass formation on the continental shelf, in *Deep Convection and Deep Water Formation in the Oceans*, edited by P. C. Chu and J. C. Gascard, *Elsevier Oceanogr. Ser.*, 57, 229–239.

Manca, B. B., V. Kovačević, M. Gačić, and D. Viezzoli (2002), Dense water formation in the Southern Adriatic Sea and spreading into the Ionian Sea in the period 1997–1999, *J. Mar. Syst.*, *33–34*, 133–154, doi:10.1016/S0924-7963(02)00056-8.

Manca, B. B., V. Ibello, M. Pacciaroni, P. Scarazzato, and A. Giorgetti (2006), Ventilation of deep waters in the Adriatic and Ionian Seas following changes in thermohaline circulation of the Eastern Mediterranean, *Clim. Res.*, *31*, 239–256.

Mantziafou, A., and A. Lascaratos (2008), Deep-water formation in the Adriatic Sea: Interannual simulations for the years 1979-1999, *Deep Sea Res., Part I*, *55*, 1403–1427, doi:10.1016/j.dsr.2008.06.005.

Marshall, J. C., A. Adcroft, C. Hill, L. Perelman, and C. Heisey (1997), A finite-volume, incompressible Navier-Stokes model for the studies of the ocean on parallel computers, *J. Geophys. Res.*, *102*, 5753–5766.

Mihanović, H., et al. (2013), Exceptional dense water formation on the Adriatic shelf in the winter of 2012, *Ocean Sci.*, *9*, 561–572, doi:10.5194/os-9-561-2013.

Oddo, P., and A. Guarnieri (2011), A study of the hydrographic conditions in the Adriatic Sea from numerical modelling and direct observations (2000–2008), *Ocean Sci.*, *7*, 549–567, doi:10.5194/os-7-549-2011.

Ovchinnikov, I. M., V. I. Zats, V. G. Krivosheya, and A. I. Idodov (1985), The formation of deep Eastern Mediterranean Waters in the Adriatic Sea, *Oceanology*, *25*, 704–707.

Prather, M. (1986), Numerical advection by conservation of second-order moments, *J. Geophys. Res.*, *91*, 6671–6681.

Querin, S., G. Cossarini, and C. Solidoro (2013), Simulating the formation and fate of dense water in a midlatitude marginal sea during normal and warm winter conditions, *J. Geophys. Res. Oceans*, *118*, 885–900, doi:10.1002/jgrc.20092.

Raicich, F., V. Malačič, M. Celio, D. Giaiotti, C. Cantoni, R. R. Colucci, B. Čermelj, and A. Pucillo (2013), Extreme air-sea interactions in the Gulf of Trieste (North Adriatic) during the strong Bora event in winter 2012, *J. Geophys. Res. Oceans*, *118*, 5238–5250, doi:10.1002/jgrc.20398.

Robinson, A. R., W. Leslie, A. Theocharis, and A. Lascaratos (2001), Mediterranean Sea circulation, in *Encyclopedia of Ocean Science*, vol. 3, pp. 1689–1706, Academic, San Diego, Calif.

Rubino, A., D. Romanenkov, D. Zanchettin, V. Cardin, D. Hainbucher, M. Bensi, A. Boldrin, L. Langone, S. Miserocchi, and M. Turchetto (2012), On the descent of dense water on a complex canyon system in the southern Adriatic basin, *Cont. Shelf Res.*, *44*, 20–29, doi: 10.1016/j.csr.2010.11.009.

Send, U., and J. Marshall (1995), Integral effects of deep convection, *J. Phys. Oceanogr.*, *25*, 855–872, 1995.

Spall, M. A. (2003), On the thermohaline circulation in flat bottom marginal seas, *J. Mar. Res.*, *61*, 1–25.

Spall, M. A. (2004), Boundary currents and water mass transformation in marginal seas, *J. Phys. Oceanogr.*, *34*, 1197–1213.

Stigebrandt, A., and J. Aure (1989), Vertical mixing in Basin waters of Fjords, *J. Phys. Oceanogr.*, *19*, 917–926.

Tsabaris, C., V. Zervakis, H. Kaberi, R. Delfanti, D. Georgopoulos, M. Lampropoulou, and C. A. Kalfas (2014), ^{137}Cs vertical distribution at the deep basins of the North and Central Aegean Sea, Greece, *J. Environ. Radioact.*, *132*, 47–56, doi:10.1016/j.jenvrad.2014.01.015.

Turchetto, M., A. Boldrin, L. Langone, S. Miserocchi, T. Tesi, and F. Foglini (2007), Particle transport in the Bari Canyon (southern Adriatic Sea), *Mar. Geol.*, *246*, 231–247, doi:10.1016/j.margeo.2007.02.007.

Vilibić, I. (2003), An analysis of dense water production on the North Adriatic shelf, *Estuarine Coastal Shelf Sci.*, *56*(3−4), 697–707, doi: 10.1016/S0272-7714(02)00277-9.

Vilibić, I., and H. Mihanović (2013), Observing the bottom density current over a shelf using an Argo profiling float, *Geophys. Res. Lett.*, *40*, 910–915, doi:10.1002/grl.50215.

Vilibić, I., and M. Orlić (2002), Adriatic water masses, their rates of formation and transport through the Otranto Strait, *Deep Sea Res., Part I*, *49*, 1321–1340.

Wang, X. H., P. Oddo, and N. Pinardi (2006), On the bottom density plume on coastal zone off Gargano (Italy) in the southern Adriatic Sea and its interannual variability, *J. Geophys. Res.*, *111*, C03S17, doi:10.1029/2005JC003110.

Zervakis, V., E. Krasakopoulou, D. Georgopoulos, and E. Souvermezoglou (2003), Vertical diffusion and oxygen consumption during stagnation periods in the deep North Aegean, *Deep Sea Res., Part I*, *50*, 53–71.